Macromolecules

ARTICLE

pubs.acs.org/Macromolecules

Aromatic Polyimides Containing Main-Chain Diphenylaminofluorene–Benzothiazole Motif: Fluorescence Quenching, Two-Photon Properties, and Exciplex Formation in a Solid State

Matthew J. Dalton,[†,‡] Ramamurthi Kannan,[†,§] Joy E. Haley,[†] Guang S. He,[∥] Daniel G. McLean,[†,⊥] Thomas M. Cooper,[†] Paras N. Prasad,[∥] and Loon-Seng Tan*[,†]

[†]Air Force Research Laboratory, Materials and Manufacturing Directorate, AFRL/RX, Wright-Patterson AFB, Ohio 45433-7750, United States

[‡]General Dynamics Information Technology, 5100 Springfield Pike, Dayton, Ohio 45431, United States

[§]AT&T Government Solutions, Inc., 2940 Presidential Drive, Suite 390, Fairborn, Ohio 45324, United States

[∥]Institute for Lasers, Photonics and Biophotonics, State University of New York at Buffalo, Buffalo, New York 14260-3000, United States

[⊥]Science Applications International Corporation, 4031 Colonel Glenn Highway, Beavercreek, Ohio 45431, United States

Supporting Information

ABSTRACT:

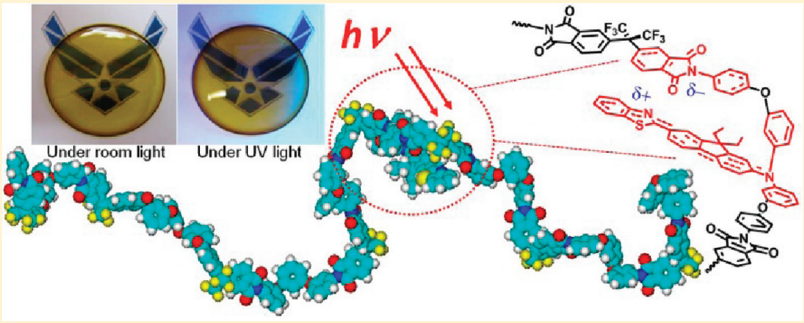

A new bis(4-aminophenoxy) monomer containing a two-photon absorbing (2PA) and fluorescent diphenylaminodiethylfluorene–benzothiazole chromophore (AF240) was synthesized and used as a comonomer in preparing a series of heat-resistant, 2PA-active polyimides. Highly organo-soluble, these polymers easily formed optically clear, but nonfluorescent, films that contained covalently bound, AF240-like dye in concentrations up to ∼1.0 M. For comparison purposes, a model compound (AF349) with phthalimido end-caps was also prepared. From the fluorescence data, the presence of phthalimido moieties in both the model compound and the polymers drastically quenched the fluorescence emission from the 2PA moieties of these materials in solution as well as in solid state. Their intrinsic (at 780 nm and with 160 fs pulses) and effective (at 800 nm and 8 ns pulses) two-photon properties in THF solutions (0.02 M), and film samples (40–65 μm thick) were determined by a direct nonlinear transmission technique. Thus, their intrinsic ($\sigma^{(2)}_{fs}$) and effective cross-section ($\sigma^{(2)}_{ns}$) values *in solution* are 7.7–37 and 1070–6000 GM per repeat unit, respectively. Surprisingly for the film samples, while the $\sigma^{(2)}_{fs}$ values agree with those determined in solutions, the $\sigma^{(2)}_{ns}$ values are 7–9 times larger, depending on the dye content. On the basis of the results of photophysical characterization of these polymers, we propose that on a nanosecond or slower time scale a stabilized/confined excited state complex is formed in an *intrachain* mode between an AF240-like moiety and a phthalimido unit to reasonably account for the fluorescence quenching and enhancement in the effective two-photon responses in film form.

INTRODUCTION

Simultaneous two-photon absorption (2PA) is a well-known phenomenon in nonlinear optics (NLO) since Göppert-Mayer's ground-breaking theoretical work 80 years ago,[1] followed by experimental verification by Kaiser and Garrett 30 years later.[2] It is related to the imaginary component of third-order susceptibility, $\chi^{(3)}$, of a nonlinear optical medium. During the early years that witnessed the development of $\chi^{(3)}$ conjugated polymers and organic materials for all-optical computing and switching applications, 2PA and related higher-order absorptive processes

Received: June 21, 2011
Revised: August 1, 2011
Published: August 25, 2011

(generically known as multiphoton absorption) along with scattering processes were considered to be problematic because of the potential loss of optical information during transmission over distance.[3] However, in comparison with one-photon absorption (1PA) and based on the fact that 2PA scales nonlinearly with the squared intensity of the incident laser beam, also recognized were several useful features: (a) near-infrared-to-visible upconverted emission; (b) deeper penetration of incident NIR light (into tissue samples, for example); (c) highly localized excitation allowing for precise spatial control of *in situ* photochemical or photophysical events; (d) amplified fluorescence by surface plasmonic resonance process.[4,5] Ostensibly, efficient two-photon materials are pivotal to the realization of many practical applications that capitalize on these features. Thus, during the past two decades, advances have been made by leaps and bounds in the design and synthesis of two-photon absorbers with very large cross-section ($\sigma^{(2)}$) values[6] that assist in expanding the range of 2PA-based application areas in photonics, nanophotonics, and biophotonics, including but not limited to bioimaging diagnostics, chemical sensing, high-density data storage, microfabrication,[7] nonlinear optical materials, photodynamic therapy, photoactivated release of NO,[8] etc.

Although two-photon dye synthesis has been the main focus during this developmental period, the synthesis of two-photon active polymers based on specifically designed monomers, with the exception of dendritic polymers,[9,10] has been receiving much less attention.[11] Among high performance heat-resistant polymers,[12] aromatic polyimides clearly stand out with a balance of polymer properties that are structurally tailored with relative ease via specific monomer designs. In addition, large-area processability via the poly(amic acid) precursor route is a unique and attractive feature. With such advantages that are important to scalability and cost considerations, polyimides are frequently found in a broad spectrum of utility,[13] ranging from lightweight, heat-resistant structural composites, adhesives, and antenna membranes for the aerospace and space sectors to gas separation membranes[14] and dielectric films and laminates, printed circuit boards, photoresists,[15] and orientation layers for electronic and photonic applications.[16] However, in the field of nonlinear optics, polyimides have been largely investigated with respect to their second-order NLO properties for electro-optical applications[17,18] and, to a lesser extent, their third-order NLO properties for optical data storage.[19−21] Thus, from the standpoint of developing multifunctional materials, aromatic polyimides are an attractive polymer platform to impart two-photon functionality.

It is well-known that excited-state absorption (ESA) plays a critical role in enhancing the properties of two-photon materials in the nanosecond regime.[22,23] However, a self-quenching process within a system that depletes the excited state population could have a negative effect on the enhanced optical nonlinearity of the material. On the other hand, if the self-quenching process leads to a new long-lived species, then an enhancement in the nonlinearity may be observed. Interestingly, while the low fluorescence and self-quenching properties of aromatic polyimides[24] are well established, the excited-state quenching phenomenon of aromatic imide moieties on the optical properties of 2PA-active polymers, to our knowledge, has not been reported.

Here, we report the results on the synthesis and optical characterization of a diamino-monomer based on the structural motif of a diphenylaminofluorene-benzothiazole-based chromophore (AF240)[25] and the resulting aromatic polyimides that are related to a well-known low-color polyimide (CP2).[26−28] These polyimides are unique in the sense that their films are both 2PA-active and nonfluorescent. Since the studies of organic and polymeric two-photon chromophores in a solid-state environment are rather sporadic, a highly organo-soluble 2PA-active polymer allows an investigation to compare and understand the fundamental relationships between polymer structure−property and two-photon processes in solution and solid state as well as the correlations between one-photon and two-photon properties influenced by these environments.

EXPERIMENTAL SECTION

Materials. All chemicals were reagent grade, purchased from Aldrich, and used as received unless otherwise noted. 7-(Benzothiazol-2-yl)-9,9-diethyl-2-bromofluorene was synthesized according to the reported procedure.[25] 2,2-Bis(phthalic anhydride)-1,1,1,3,3,3-hexafluoroisopropane (6-FDA; 99%) was purified by sublimation and stored in a desiccator before use; 1,3-bis(3-aminophenoxy)benzene (APB) was (99% min) was used as received. Both monomers were purchased from Chriskev Co., Inc.

Instrumentation. NMR spectra were obtained using a Bruker Avance 400 MHz spectrometer, and chemical shifts were referenced to the solvent residual peak. Elemental analyses and mass spectral analyses were performed at the Systems Support Branch, Materials & Manufacturing Directorate, Air Force Research Lab, Dayton, OH. Melting points were obtained on either a Buchi-B545 melting point apparatus or a MelTemp apparatus. Polymer molecular weights were determined by GPC using a PL-Gel mixed-C column and RI detector with THF at a flow rate of 1.0 mL/min. Conventional calibration against polystyrene standards was used. Intrinsic viscosities [η] were measured using a Cannon-Ubbelohde dilution viscometer with an initial concentration of ~0.5 g/dL in NMP (1 wt % LiBr) at 30 ± 0.1 °C. Differential scanning calorimetry (DSC) analyses were performed in nitrogen at a heating rate of 10 °C/min using a TA Instruments Q1000 differential scanning calorimeter. Thermogravimetric analyses (TGA) were obtained in nitrogen and air atmospheres at a heating rate of 10 °C/min using a TA Hi-Res TGA 2950 thermogravimetric analyzer.

***N,N*-Di(3-methoxyphenyl)-7-(benzothiazol-2-yl)-9,9-diethylfluoren-2-amine (2).** A mixture of 7-(benzothiazol-2-yl)-9,9-diethyl-2-bromofluorene (10.85 g, 25 mmol), 3,3′-dimethoxydiphenylamine (6.87 g, 30 mmol), and toluene (100 mL) was azeotroped dry under nitrogen and cooled. Bis(dibenzylidene acetone)palladium(0) (0.28 g, 0.49 mmol), bis(diphenylphosphino)ferrocene (0.25 g, 0.45 mmol), and sodium *tert*-butoxide (3.5 g, 36.4 mmol) were then added, and the mixture was heated to 100 °C. After 24 h at 100 °C, the mixture was cooled, diluted with toluene, and filtered. The filtrate was washed with water, dried, and concentrated on a rotary evaporator. The residue was chromatographed over silica gel. Elution with toluene−heptane (3:1) mixture gave the product, which was recrystallized from a mixture of toluene−heptane; mp 178−179.5 °C, 11.13 g (76% yield). ^{1}H NMR ($CDCl_3$) δ ppm: 0.35−0.41 (t, 6H), 1.91−2.14 (m, 4H), 3.69 (s, 6H), 6.54−6.74, 7.05−7.68, 7.84−8.10 (m, 18H). ^{13}C NMR ($CDCl_3$) δ ppm: 8.61, 32.66, 55.18, 56.44 (sp^3 C), 108.62, 109.77, 116.66, 119.16, 119.42, 121.00, 121.44, 121.52, 122.94, 123.77, 124.95, 126.28, 127.28, 129.82, 131.55, 134.91, 135.61, 144.48, 147.84, 148.94, 150.67, 151.99, 154.24, 160.46, 168.81 (sp^2C). Anal. Calcd for $C_{38}H_{34}N_2O_2S$: C, 78.33%; H, 5.88%; N, 4.81%; S, 5.49%. Found: C, 78.26%; H, 5.96%; N, 4.68%; S 5.47%.

***N,N*-Di(3-hydroxyphenyl)-7-(benzothiazol-2-yl)-9,9-diethylfluoren-2-amine (3) [AF240-(OH)$_2$].** A mixture of *N,N*-di(3-methoxyphenyl)-7-(benzothiazol-2-yl)-9,9-diethylfluoren-2-amine (1 g) and pyridine hydrochloride (10 g) was heated at 200 °C under a nitrogen atmosphere in an oil bath for 10 h. The reaction mixture was allowed to cool to room temperature and slurried in water, and the red

solids were collected on a fritted filter funnel. The crude (protonated) red product was subsequently slurried in dilute ammonium hydroxide to get the greenish-yellow solid product; 1.13 g, mp 314−316 °C. EIMS: m/z 554 (M^+). Anal. Calcd for $C_{36}H_{30}N_2O_2S$: C, 77.95%; H, 5.45%; N, 5.05%; S, 5.78%. Found: C, 77.74%; H, 5.39%; N, 4.83%; S, 5.78%.

7-(Benzo[*d*]thiazol-2-yl)-9,9-diethyl-*N*,*N*-bis(3-(4-nitrophenoxy)phenyl)-9*H*-fluoren-2-amine (4a) [AF240(PhNO$_2$)$_2$]. A mixture of AF240-(OH)$_2$ (2.94 g, 5.3 mmol), 4-nitrofluorobenzene (2.56 g, 20 mmol), potassium carbonate (2.29 g, 16.6 mmol), and *N*,*N*-dimethylacetamide (DMAc; 27 mL) was heated at 97 °C for 5 h, allowed to cooled to room temperature, and poured into water. The separated solids (4.38 g) were transferred to a column of silica gel and eluted with toluene to get the product; 4.12 g (97% yield), mp 200−201 °C. Recrystallization from toluene−heptane provided a purer sample with mp 202−203 °C. ^{1}H NMR (400 MHz, $CDCl_3$) δ 8.15−8.22 (m, 4H), 8.07−8.12 (m, 2H), 8.02 (dd, J_1 = 7.9 Hz, J_2 = 1.6 Hz, 1H), 7.91 (d, J = 7.9 Hz, 1H), 7.72 (d, J = 7.9 Hz, 1H), 7.68 (d, J = 8.1 Hz, 1H), 7.45−7.55 (m, 1H), 7.36−7.42 (m, 1H), 7.31 (t, J = 8.1 Hz, 2H), 7.12−7.2 (m, 2H), 6.98−7.05 (m, 6H), 6.89 (t, J = 2.2 Hz, 2H), 6.72−6.77 (m, 2H), 1.88−2.15 (m, 4H), 0.31 (t, J = 7 Hz, 6H). ^{13}C NMR (100 MHz, $CDCl_3$) δ 168.52, 162.96, 155.53, 154.15, 152.45, 150.66, 149.23, 146.49, 143.77, 142.63, 137.09, 134.90, 132.07, 130.83, 127.32, 126.31, 125.90, 125.05, 124.54, 122.97, 121.55, 121.47, 121.40, 120.19, 120.09, 119.73, 117.00, 115.47, 114.66, 56.49, 32.61, 8.55. MS (m/z): 796 (M^+). Anal. Calcd for $C_{48}H_{36}N_4O_6S$: C, 72.35; H, 4.55; N, 7.03; S, 4.02. Found: C, 72.15; H, 4.87; N, 6.87; S, 3.95.

***N*,*N*-Bis(3-(4-aminophenoxy)phenyl)-7-(benzo[*d*]thiazol-2-yl)-9,9-diethyl-9*H*-fluoren-2-amine (4b) [AF240(PhNH$_2$)$_2$].** To a solution of AF240(PhNO$_2$)$_2$ (13.68 g, 17.2 mmol) in 300 mL of 1/1 tetrahydrofuran/ethanol under argon was added 10% palladium/carbon (500 mg). The mixture was heated to 60 °C, and hydrazine hydrate (12.7 mL, ∼206 mmol) was added slowly over 40 min via an addition funnel. The reaction mixture became dark, fluorescent green and, after 8 h, was cooled to room temperature and poured into 1.5 L of distilled water. After a few hours of stirring to evaporate some THF in a well-ventilated hood, a fine yellow solid was filtered and purified by column chromatography eluting with 20−50% ethyl acetate/toluene. Three byproducts generated in the reaction and separated by column chromatography were identified by mass spectrometry as the following compounds:

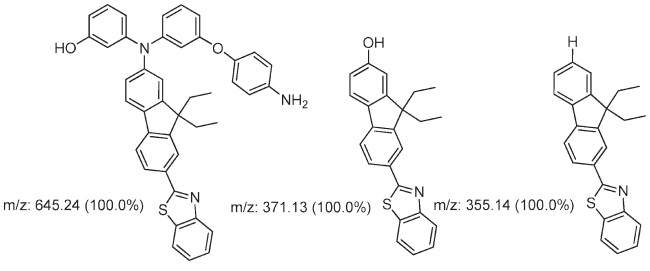

It is not clear how the byproduct m/z 645 was produced in the reaction, and it was also particularly difficult to remove by column chromatography. The product was further slurried in 100 mL of hot EtOH, filtered at room temperature, and dried *in vacuo* at 70 °C overnight to give 8.4 g (65% yield) of the desired diamine product (1 spot on TLC); mp 170−171 °C (in a separate DSC experiment, a sharp melting endotherm was observed at 170 °C, which was preceded by a somewhat broad endotherm staring at ∼137 °C when a sample was scanned under N_2 and at 20 °C/min). ^{1}H NMR (400 MHz, $CDCl_3$) δ 8.08 (m, 2H), 8.01 (dd, J_1 = 8 Hz, J_2 = 1.6 Hz, 1H), 7.91 (d, J = 8 Hz, 1H), 7.70 (d, J = 8 Hz, 1H), 7.48−7.55 (m, 1H), 7.35−7.42 (m, 1H), 7.05−7.18 (m, 4H), 6.52−6.59 (m, 2H), 3.5−3.6 (br. s, 4H), 1.95−2.15 (m, 4H), 0.34 (t, J = 7 Hz, 6H). ^{13}C NMR (100 MHz, $CDCl_3$) δ 168.97, 159.73, 154.38, 152.23, 150.91, 149.04, 148.61, 147.69, 144.56, 142.72, 135.98, 135.07, 131.71, 129.98, 127.39, 126.42, 125.11, 124.19, 123.08, 121.68, 121.59, 121.19, 121.00, 119.60, 119.54, 117.90, 116.31, 113.33, 111.70, 56.57, 32.77, 8.73; MS (m/z): 736 (M^+). Anal. Calcd for $C_{48}H_{40}N_4O_2S$: C, 78.23; H, 5.47; N, 7.60; S, 4.35. Found: C, 78.01; H, 5.60; N, 7.62; S, 4.31.

Model Compound 5 (AF349); 2,2′-(((((7-(Benzo[*d*]thiazol-2-yl)-9,9-diethyl-9*H*-fluoren-2-yl)azanediyl)bis(3,1-phenylene))bis(oxy)bis(4,1-phenylene))diisoindoline-1,3-dione. To a 25 mL flame-dried vial equipped with a magnetic stir bar was added **4b** (0.425 g, 0.577 mmol), and the vial was sealed with a Teflon-coated septum cap. Anhydrous DMAc (5 mL) was added by a hypodermic syringe to give a fluorescent solution. Phthalic anhydride (0.180 g, 1.21 mmol) was added under a stream of argon, and the vial was sealed. After 40 h, acetic anhydride (0.22 mL) and pyridine (0.19 mL) were added, and the mixture was stirred for another 24 h. The product was precipitated upon adding the reaction mixture to 50/50 methanol/water (50 mL) and collected after filtration. The product was then slurried in isopropanol/methanol, filtered, and finally dried *in vacuo* at 120 °C overnight to give 0.53 g (92%) of the product. ^{1}H NMR (400 MHz, $CDCl_3$) δ 8.13−8.04 (m, 2H), 8.00 (dd, J = 7.9, 1.3 Hz, 1H), 7.98−7.86 (m, 5H), 7.82−7.74 (m, 4H), 7.72 (d, J = 7.9 Hz, 1H), 7.67 (d, J = 8.1 Hz, 1H), 7.50 (dd, J = 11.3, 4.0 Hz, 1H), 7.46−7.34 (m, 5H), 7.34−7.22 (m, 2H), 7.22−7.06 (m, 6H), 7.01−6.87 (m, 4H), 6.72 (dd, J = 8.1, 1.7 Hz, 2H), 2.11 (dq, J = 14.1, 7.1 Hz, 2H), 1.97 (dq, J = 14.5, 7.2 Hz, 2H), 0.35 (t, J = 7.3 Hz, 6H). ^{13}C NMR (100 MHz, $CDCl_3$) δ 168.93, 167.46, 157.38, 157.07, 154.35, 152.42, 150.94, 149.27, 147.30, 144.40, 136.48, 135.06, 134.50, 131.84, 130.49, 128.09, 127.38, 126.47, 126.40, 125.10, 124.32, 123.86, 123.07, 121.68, 121.59, 121.42, 119.82, 119.75, 119.41, 118.78, 115.32, 113.98, 56.63, 32.80, 8.74. EI-MS (m/z): 997 (M^+). Anal. Calcd for $C_{64}H_{44}N_4O_6S$: C, 77.09; H, 4.45; N, 5.62; S, 3.22; Found: C, 76.83; H, 4.47; N, 5.47; S, 3.14.

Homopolyimide Synthesis (7e). To a 25 mL flame-dried vial equipped with a magnetic stir bar was added **4b** (1.4738 g, 2.00 mmol), and the vial was sealed with a Teflon-coated septum cap. Anhydrous DMAc (15 mL) was added by a hypodermic syringe to give a fluorescent solution. 6-FDA (0.8885 g, 2.00 mmol) was then added under a stream of argon, and the vial was sealed under argon. After 40 h, acetic anhydride (0.75 mL) and pyridine (0.65 mL) were added, and the mixture was stirred for 24 h. The viscous solution was precipitated into 50/50 methanol/water (200 mL), and the yellow, fibrous solid was filtered and dried at 120 °C overnight in a vacuum oven. The solid was dissolved in chloroform (25 mL) and filtered through a 0.45 μm PTFE membrane directly into methanol (200 mL). The purified polymer was dried *in vacuo* at 120 °C overnight and further at 250 °C for 2 h to yield 1.99 g (87%). ^{1}H NMR (400 MHz, $CDCl_3$) δ 7.8−8.1 (m, 10H), 7.7 (d, J = 8 Hz, 1H), 7.65 (d, J = 8.1 Hz, 1H), 7.45−7.52 (m, 1H), 7.32−7.40 (m, 5H), 7.22−7.30 (m, 2H), 7.08−7.20 (m, 6H), 6.88−6.98 (m, 4H), 6.68−6.74 (m, 2H), 1.90−2.20 (m, 4H), 0.34 (t, J = 7 Hz, 6H). ^{13}C NMR (100 MHz, $CDCl_3$) δ 168.75, 166.17, 166.01, 157.35, 157.04, 154.19, 152.32, 150.79, 149.17, 147.08, 144.20, 139.10, 136.45, 135.90, 134.90, 132.62, 132.33, 131.74, 130.40, 127.93, 127.27, 126.29, 125.80, 125.29, 125.00, 124.22, 124.11, 122.93, 121.54, 121.46, 121.31, 119.73, 119.63, 119.40, 118.62, 115.29, 113.97, 65.50, 56.50, 32.66, 8.60.

Representative Copolyimide Synthesis (7d). To a 25 mL flame-dried vial equipped with a magnetic stir bar was added **4b** (0.7368 g, 1.00 mmol) and 1,3-bis(3-aminophenoxy)benzene (0.2923 g, 1.00 mmol), and the vial was sealed with a Teflon-coated septum cap. Anhydrous DMAc (13 mL) was added by syringe to give a fluorescent solution. 6-FDA (0.8885 g, 2.00 mmol) was added under a stream of argon, and the vial was sealed. After 27 h, acetic anhydride (0.75 mL) and pyridine

Scheme 1. Syntheses of Diamine Monomer (4) and Model Compound (5)[a]

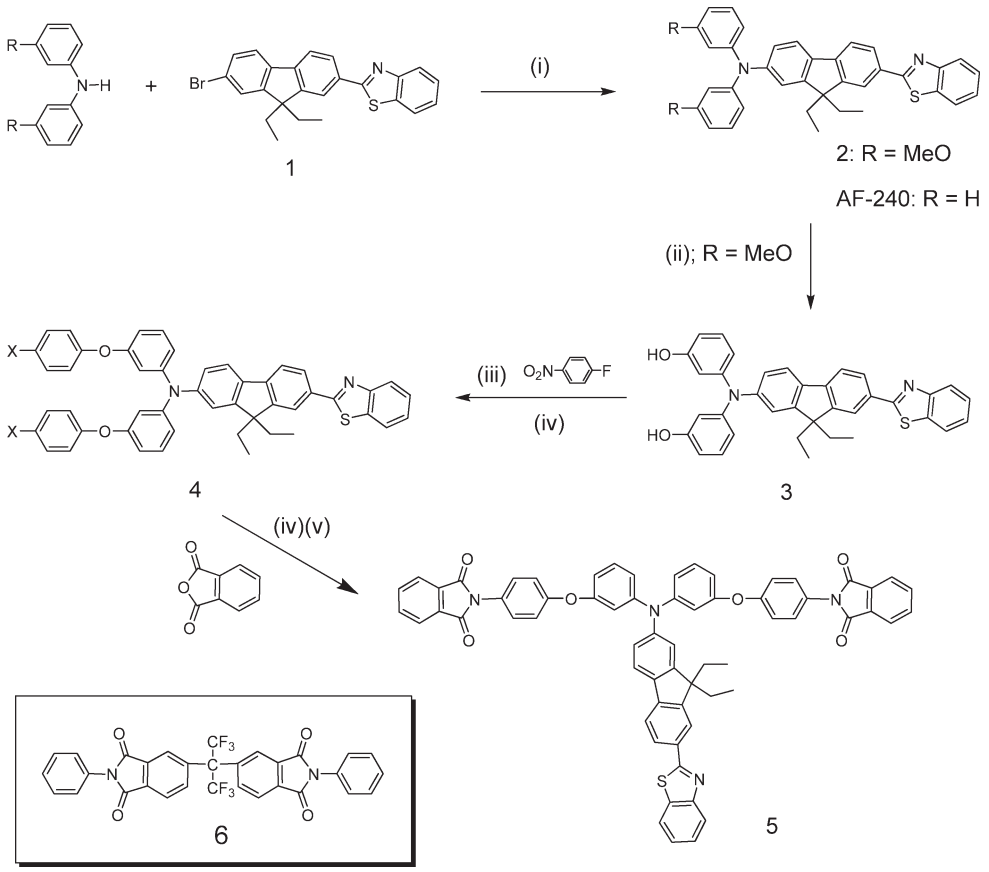

[a] Reagents and conditions: (i) Pd catalyst, *tert*-BuONa, PhMe; (ii) pyridine hydrochloride, 200 °C; (iii) K_2CO_3/DMAc; (iv) $NH_2NH_2.H_2O$, Pd/C, EtOH/THF; (v) DMAc; Ac_2O/pyridine. Inset shows chemical structure for model compound **6**.

(0.65 mL) were added, and the mixture was stirred for 24 h. The viscous solution was precipitated into 50/50 methanol/water (200 mL), and the yellow, fibrous solid was filtered and dried at 120 °C overnight in a vacuum oven. The solid was dissolved in chloroform (25 mL) and filtered through a 0.45 μm PTFE membrane directly into methanol (200 mL). The purified polymer was dried *in vacuo* at 120 °C overnight and further at 250 °C for 2 h to yield 1.60 g (87%). Anal. Calcd for $C_{52}H_{30}F_6N_3O_6S_{0.5}$(repeat unit): C, 67.68; H, 3.28; N, 4.55; S, 1.74; Found: C, 67.56; H, 3.31; N, 4.29; S, 1.68.

CP2 Polyimide Film Density Determination and Dye Concentration Calculation. Small pieces of CP2 polyimide films were suspended individually in a mixture of carbon tetrachloride and ethanol in a 10 mL graduated cylinder which had previously been tarred. The total solvent volume was between 9.4 and 10 mL, and the films were suspended around the 5 mL mark when the solvent was weighed. The mass of the solution and the total volume were used to calculate a density. The films did not swell in the solvent mixture.

Dye concentrations were calculated based on the following equation, assuming the model compound (AF-349) structure as the "dye" fragment (FW = 995 g/mol):

$$\text{conc [M]} = \text{density}\left(\frac{\text{g}}{\text{mL}}\right)\left(\frac{1000\ \text{mL}}{\text{L}}\right)\left(\frac{\text{mol}}{\text{repeat unit mol wt}}\right)\left(\frac{995\ \text{g/mol}}{1145\ \text{g/mol}}\right)(\%\ \text{dye})$$

The resulting density values and corresponding 2PA dye concentrations for polyimide films **7a**−**7e** are given in Table S-1 of the Supporting Information.

One-Photon Absorption and Emission Characterization. A Cary 500 spectrophotometer was used to obtain the ground-state UV/vis absorption spectra. These spectra were then used to obtain molar absorption coefficients by applying Beer's law to particular wavelengths for comparison across the samples. Ground-state spectra were run twice in which each run had a new solution prepared. All techniques mentioned herein were performed under air-saturated conditions.

The emission spectra were obtained from a Perkin-Elmer model LS 50B fluorometer. Each solution sample was excited at 355 nm with a matched OD of 0.1 with a 1 cm path length. Fluorescence quantum yields were determined by using the relative actinometry method.[29] The actinometer used is quinine sulfate, which has a known fluorescence quantum yield of 0.546 in 1.0 N H_2SO_4.[30]

Emission measurements of the film samples were done at 400 nm using a front-face geometry to eliminate any inner filter effects that might be caused by the high absorbance at the exciting wavelength. Despite the large emission observed in solution, weak emission was detected for these samples.

Time-correlated single photon counting (Edinburgh Instruments OB920 spectrometer) was used to determine singlet excited-state lifetimes. The fluorescence was excited using a 70 ps laser diode at 375 nm. The emission was detected using a cooled microchannel plate PMT. Data were analyzed using a deconvolution software package provided by Edinburgh Instruments.

Two-Photon Cross-Section Determination. Since the linear absorption peaks of all the samples are located below the 450 nm (see Figure 4) spectral range, and the residual linear absorption influences are entirely negligible around the 800 nm range, any measured intensity-dependent nonlinear absorption in the latter wavelength range should be

Scheme 2. Poly(amic acid) Formation Followed by Chemical Imidization To Give Polymers 7a−e[a]

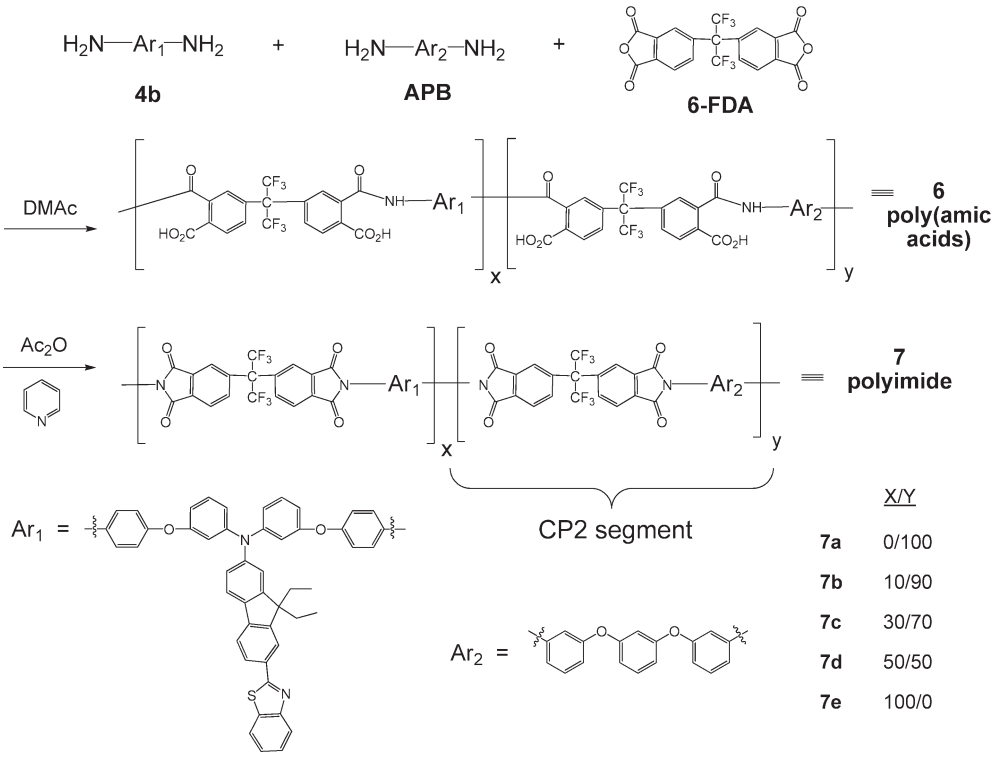

[a] General scheme for the preparation of two-photon active polyimides and their poly(amic acid) precursors.

mainly ascribed to a two-photon absorption (2PA) process. In this work, the 2PA coefficient (dependent on the concentration of absorbing center) was directly measured using a nonlinear transmission (NLT) method. Knowing the 2PA coefficient (β) and sample's concentration, the 2PA cross-section value of each absorbing center (molecule or repeat unit) was finally extracted. For the 2PA measurement performed in the femtosecond regime, the input pulsed Ti:sapphire laser beam of ~780 nm wavelength, ~160 fs pulse duration, and 1 kHz repetition rate was focused into the center of the sample cuvette via an $f = 20$ cm lens.[31] In order to avoid the possible thermal-lensing effect or boiling of the solvent due to light-absorption-induced heating, the laser beam was passed through a beam chopper with an opening/blocking ratio of 1:10 before entering the focusing lens, so that the effective pulse repetition rate (as well as the heating effect) was reduced by 10 times. For a fixed sample position, the nonlinear transmission was measured as a function of laser pulse intensity (or energy) that was controlled by a variable attenuator and was varied from 0.1 to 1.1 μJ. On the basis of this type of nonlinear transmission measurement, the 2PA coefficient was readily determined.

The same experimental setup and procedure were applied to perform 2PA measurements in the nanoseconds regime, where the input pulsed laser beam of ~800 nm wavelength, ~8 ns pulse duration, and 10 Hz repetition rate was from a tunable-dye laser pumped by a frequency-doubled and Q-switched Nd:YAG laser device.[32] However, in this case the pulse energy was much greater (from 0.1 to 1.3 mJ).

AF350 was used as a calibration standard (0.01 M THF solution in 10 mm cuvette) for all NLT measurements. In this work, femtosecond β value of 0.0306 cm/GW and nanosecond β value of 5.16 cm/GW were obtained, which agree well with those reported previously.[33]

RESULTS AND DISCUSSION

Monomer and Model Compound Syntheses. Since a previously reported two-photon chromophore designated as AF240 has a relatively high effective (nanosecond) two-photon cross section, its multistep synthesis[25] has been optimized, it has been subject to several theoretical and modeling studies,[23,34,35] and it should serve well to probe the subtle effects of polymer architecture on the 2PA responses. Thus, to incorporate it into an aromatic diamine that could be conveniently synthesized and polymerized, we chose to functionalize it at the 3,3′-positions of the diphenylamino donor, partly because of the commercial availability of 3,3′-dimethoxydiphenylamine. In addition, ether spacers at the meta positions of the phenyl rings would provide additional structural flexibility for improved solubility.

Thus, the 3,3′-dihydroxy derivative of AF240, i.e., AF240-$(OH)_2$ (**3** in Scheme 1), was prepared from a standard Pd-catalyzed N-arylation of 3,3′-dimethoxydiphenylamine with a previously reported intermediate, benzothiazole−diethylfluorenyl bromide (**1**),[25] followed by a double demethylation through the agency of pyridinium chloride. The dinitro precursor, AF240-$(PhNO_2)_2$, to the requisite diamine monomer was subsequently synthesized from AF240$(OH)_2$ and 4-nitrofluorobenzene via a nucleophilic aromatic substitution in excellent yield (97%). However, a subsequent catalytic reduction of the dinitro compound to give the desired monomer AF240$(PhNH_2)_2$, **4b**, using standard Parr hydrogenator conditions (H_2−10% Pd/C) proved to be problematic as the solubility of AF240$(PhNO_2)_2$ in alcoholic solvents was poor. The reaction proceeded very sluggishly in THF/ethanol solvent to give a mixture of AF240$(PhNH_2)_2$, monoreduced product, and an unidentified byproduct seen by TLC analysis. Thus, we turned to transfer hydrogenation with hydrazine hydrate, which proceeded more smoothly to generate AF240$(PhNH_2)_2$, that was obtained after column chromatography as a yellow solid in reasonable yield (62%). ^{1}H and ^{13}C NMR spectroscopy, electron-impact mass spectroscopy, and elemental

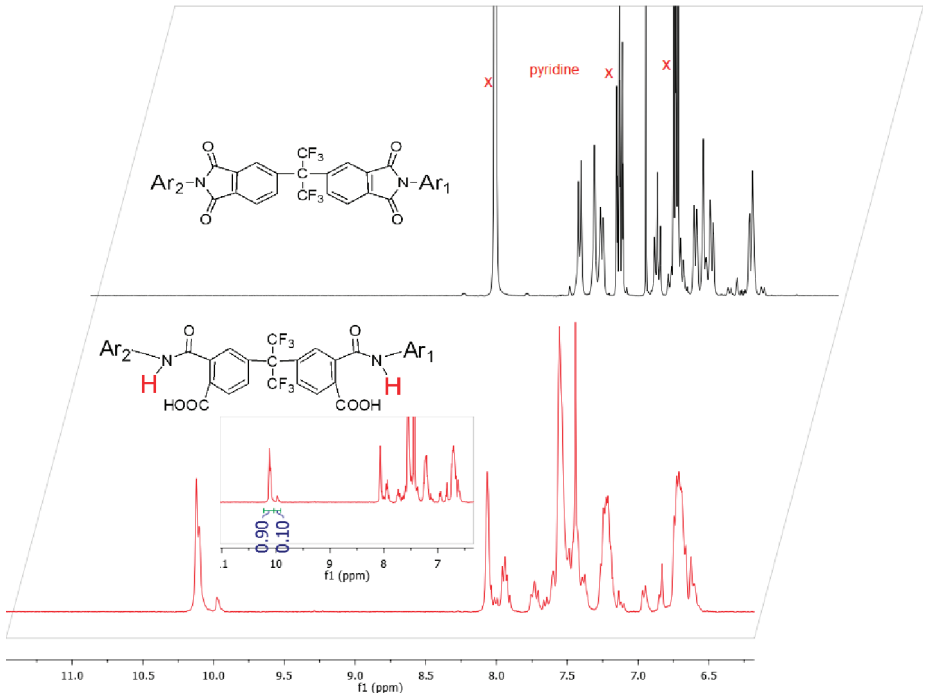

Figure 1. NMR spectra taken before (bottom) and after (top) chemical imidization of 90/10 copolymer (**7b**), with inset showing amic acid proton ratios. The peaks due to the proton residues of pyridine-d_5 solvent are indicated by X's.

analysis were consistent with the expected structure for the diamino monomer.

In order to evaluate the contribution of polymer architecture as well as the influence of phthalimide functionality on the one- and two-photon properties of the subject polyimides, a model compound (**5** and designated as AF349 in Scheme 1) was synthesized by end-capping AF240($PhNH_2$)$_2$ with phthalic anhydride.

Polymer Synthesis. The subject CP2-based polyimide (AF349P) and copolymers (AF349P-XXCP2) were prepared as depicted in Scheme 2.[36] Thus, the poly(amic acid) precursors were formed by stirring the appropriate monomers 1,3-bis(3-aminophenoxy)benzene (APB), and 6FDA in anhydrous DMAc for 24−36 h, followed by chemical imidization with a mixture of acetic anhydride and pyridine (4 equiv) at room temperature for 24 h. The AF240(NH_2)$_2$ comonomer (**4b**) content was varied between 0 and 100% to give polyimides **7a**−**e** in purified yields of 80−90%.

An attractive feature of these polyimides is their excellent solubility in common organic solvents such as THF, DMAc, DMF, NMP, and DMSO. Therefore, NMR spectroscopy is a convenient method to follow the course of the imidization reaction, i.e., the cyclo-dehydration of the amic acid group. For example, in the ^{1}H NMR spectrum as shown in Figure 1 for AF349-10CP2 (**7b**), the amic acid (N−H) proton signals at ~10.0 ppm are completely gone after chemical imidization. The amic acid proton adjacent to Ar_1, i.e., in the 2PA-active segment, at 9.97 ppm was slightly upfield from TMS standard but clearly separated from the amic acid proton near Ar_2, i.e., in the "CP2" segment, at 10.10 ppm. The integrations of these two protons compare well with the molar feed ratio (**4b**:APB); see inset in Figure 1. This result, along with the elemental analysis data shown in Table 1, is a good indicator that the feed ratio is very close to the final copolymer composition.

The molecular weights (MW) of resulting polymers were characterized by size-exclusion chromatography (GPC) in THF against the polystyrene standards. GPC results (Table 1) indicated that the number-averaged MW (M_n) values vary between 99 and 40 kDa with polydispersity (PDI) range of 1.87−2.36, corresponding to the degrees of polymerization (DP) range of 35−141. Polymers **7a**, **7b**, and **7c** formed tough, creasable, and optically transparent films from their chloroform or DMAc solutions. The films of **7d** and **7e** were optically transparent, but somewhat brittle due to the lower molecular weights. The GPC results indicate that as the content of chromophore is increased, the polymer molecular weight decreases. This is most likely due to the sensitivity of polymer-growing process to the mass imbalance as the monomer **4b** is an amorphous solid, which was found to be very difficult to obtain in ultrahigh purity necessary for exact stoichiometry in the polycondensation reaction.

The molecular weights of the polymer samples were further corroborated using viscometry in NMP at 30 ± 0.1 °C with 1 wt % LiBr. The intrinsic viscosity ($[\eta]$) values ranged from 1.31 to 0.70 dL/g (Table 2). We observed that some samples displayed polyelectrolyte effects at dilute concentrations even with 1 wt % LiBr. Therefore, $[\eta]$ was estimated using the viable data points at higher concentrations. The linear relationship between log($[\eta]$) and log(M) (based on Mark−Houwink−Sakurada (MHK) equation, $[\eta] = KM^a$; see Figure S-1) still holds, even though the polymer composition is changing, which suggests that the solution properties for the copolymers are very similar. The plot gives an a value of 0.53, which corresponds to a flexible polymer in a theta solvent.

Thermal Properties. The polymers were characterized by differential scanning calorimetry (DSC) and thermogravimetric analysis (TGA) in both nitrogen and air atmospheres, and their glass transition (T_g) and decomposition temperatures are noted in Table 1. Experimentally, the samples were heated to 300 °C in the DSC chamber in the first run and then cooled to ambient temperature at 10 °C/min under a steady nitrogen purge. Then

Table 1. Elemental Analysis and Thermal Properties for 7a−e

			elemental analyses						
polymer	mol formula (mol wt)		C	H	N	S	T_g[a] (°C)	T_d[b] (5%) N_2/air (°C)	dye[c] conc (M)
7a	$C_{37}H_{18}F_6N_2O_6$	calc	63.44	2.59	4.00	N/A	208	527	0.00
	700.57	found	63.12	2.74	3.87			516	
7b	$C_{40}H_{20.4}F_6N_{2.2}O_6S_{0.1}$	calc	64.49	2.76	4.14	0.43	211	522	0.17
	745.03	found	64.38	2.80	3.94	0.60		500	
7c	$C_{46}H_{25.2}F_6N_{2.6}O_6S_{0.3}$	calc	66.25	3.05	4.37	1.15	217	513	0.44
	833.95	found	65.85	3.19	4.22	1.19		502	
7d	$C_{52}H_{30}F_6N_3O_6S_{0.5}$	calc	67.68	3.28	4.55	1.74	223	506	0.63
	922.87	found	67.56	3.31	4.29	1.68		498	
7e	$C_{67}H_{42}F_6N_4O_6S$	calc	70.27	3.70	4.89	2.80	241	500	0.99
	1145.17	found	70.48	3.89	4.74	2.80		500	

[a] Inflection point in baseline of DSC at heating rate of 10 °C/min in N_2. [b] Decomposition temperature at 5 wt % loss from TGA (10 °C/min) in N_2 and air. [c] Dye (AF349) concentrations in polymer samples are calculated as described in the Experimental Section.

Table 2. Molecular Weight Characterization for Polyimides 7a−e

polymer	M_w (kDa)	M_n (kDa)	PDI	DP	$[\eta]$ (dL/g)
7a	222	99	2.24	141	1.31
7b	212	90	2.36	121	1.14
7c	121	54	2.24	65	0.91
7d	94	47	1.98	51	0.77
7e	75	40	1.87	35	0.70

the samples were heated to 300 at 10 °C/min in the second run. The T_g's were determined based on the midpoint of change in slope on the second heating run. As would have been expected, the bulky chromophoric (AF-349-like) units extending from the polymer backbone make the segmental and long-range molecular motions more difficult and, therefore, increase the T_g (Figure 2). Indeed, the DSC results have confirmed that the T_g increases monotonously from 208 to 241 °C as the mole percentage of AF-349 units varies from 0 to 100% per repeat unit in the polymer compositions.

According to TGA results (Figure 3), these polymers could be considered to be very thermally and thermo-oxidatively stable under short-term extreme conditions, as their decomposition temperatures (5% weight loss; $T_{d5\%}$) are at or above 500 °C in both air and inert conditions.

Polymer Film Thickness & Density. For optical characterization of the polymer film samples, the information on the film thickness (equivalent to optical path length) and density is required. The concentration of 2PA unit in a polymer film can be calculated once the film density is determined experimentally. Thus, the thickness of each tested film sample was measured by using a micrometer caliper with an uncertainty of ±2.5 μm. The density of each polymer film[37] was determined based on Davy's principle of hydrostatic suspension using a mixture of carbon tetrachloride and ethanol as the suspension medium. The values of 1.30−1.43 g/cm^3 for **7e**-**7b** (Table S-1, Supporting Information) correspond to dye (structurally equivalent to AF349 model compound, **5**) concentrations ranging from 0.17 to 0.99 M in the solid state. This is tantamount to 1−2 orders of magnitude higher than what is achievable in dye-saturated solutions or by doping an optically transparent, polymeric host such as PMMA with AF240.

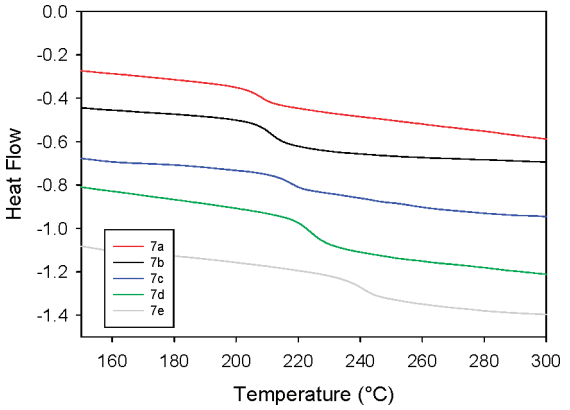

Figure 2. DSC thermograms for polyimides **7a**−**7e**.

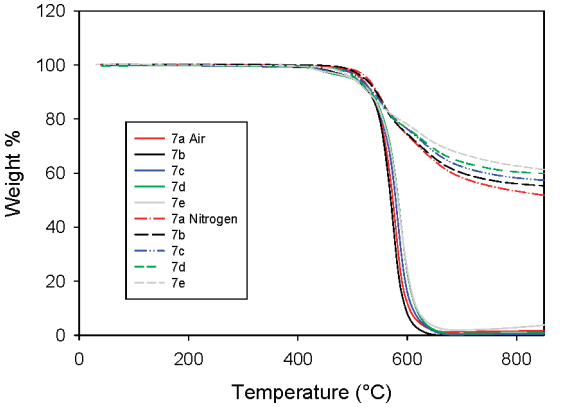

Figure 3. TGA traces of polyimides **7a**−**7e** in nitrogen and air.

One-Photon Absorption and Fluorescence Properties (Table 3). The quantified UV/vis spectra in air-saturated THF of the model compound **5**, the homopolymer **7e**, and the copolymers **7a**−**7d** are shown in Figure 4. The molar absorption coefficient (ε_{max}) of the model compound **5** (AF349) was found to be 48 030 ± 700 M^{-1} cm^{-1} at 385 nm as opposed to 39 600 ± 300 M^{-1} cm^{-1} at 384 nm for **7e** (Figure 4). The UV/vis spectra for the copolymers (**7a**−**7d**) are similar to that of homopolymer **7e**, except

Table 3. Photophysical Properties of AF240, Model Compound (AF349), and Polyimides 7a−7e[a]

sample	Abs (λ_{max}), nm	ε, M^{-1} cm^{-1}	Fl (λ_{max}), nm	Φ_{fl}[b]	τ_{s1}[c]	τ_{s2}[c]
7a THF	304	2930 ± 20				
7b THF	384	4380 ± 30	463	0.0719 ± 0.004	100 ps (25%)	404 ps (75%)
7c THF	384	12700 ± 160	463	0.0683 ± 0.004	125 ps (33%)	420 ps (67%)
7d THF	384	20500 ± 300	463	0.0712 ± 0.004	130 ps (36%)	415 ps (64%)
7e THF	384	39600 ± 300	463	0.0660 ± 0.004	111 ps (30%)	364 ps (70%)
AF240 THF	391	44400 ± 2200	475	0.748 ± 0.040	2.17 ns	
5 (AF349)	385	48030 ± 700	464	0.200 ± 0.001		
7a film						
7b film			631		1.63 ns (7%)	13.3 ns (93%)
7c film			639		1.63 ns (11%)	11.9 ns (89%)
7d film			629		1.52 ns (13%)	10.7 ns (87%)
7e film			632		1.52 ns (15%)	10.3 ns (85%)

[a] Data were obtained in air-saturated THF solutions and thin film samples. [b] Quantum yield error is standard deviation from multiple measurements. Measurements were done under air saturated conditions. [c] Lifetimes measured under air saturated conditions. Percentage values given are the contribution of the lifetime to the overall biexponential decay.

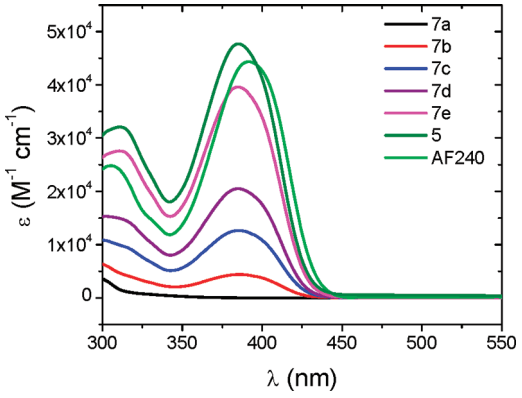

Figure 4. UV−vis spectra of polyimides **7a**−**7e**, the model compound **5**, and AF240 reference compound in air-saturated THF. Data were quantified using the Beer's law method.

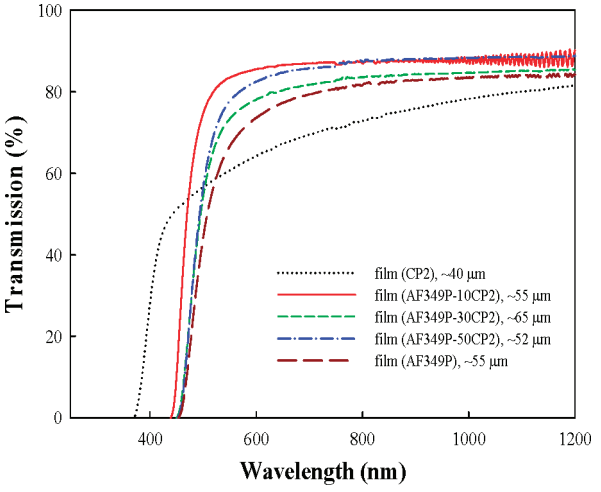

Figure 5. Linear transmission spectra of polymer **7a**−**7e** film samples. See Table 4 also.

for the band intensity at 384 nm, which varies proportionately to the AF240 content. The absorption band at 384 nm was found to be slightly blue-shifted (6−7 nm) from that of the AF240 molecule (see Figure 4). The meta substitution of ether oxygen generally has an inductive electron-withdrawing effect as evidenced by the slightly positive Hammet parameter (σ = +0.10).[38] This stabilizes the HOMO relative to AF240[39] and causes the blue shift in absorption.

Solid-state linear transmission spectra (Figure 5) were taken for the polymer **7a**−**7e** films with their thickness ranging from ~40 to 65 μm. Except for film **7a** (CP2), all 2PA-active film samples showed good optical transparency for the spectral range 700 −1200 nm.

The steady-state emission of the model compound and polymers in air-saturated THF was monitored after excitation at 355 nm (Figure 6). The absorbance at 355 nm was nearly matched to be 0.1 at the excitation wavelength for the polymer samples. For the model compound **5** and AF240, the data has been normalized for comparison. All the polymers and model compound (AF349) in THF show a peak at 463 nm, which is slightly blue-shifted from the reference compound (AF240), which has a maximum at 475 nm. This blue shift is also in agreement with a stabilized HOMO level relative to that of AF240. The LUMO is most likely unchanged by the ether oxygen substitution at the donor end because it is localized on the benzothiazole acceptor moiety.[39]

Fluorescence quantum yields were determined using quinine sulfate as a reference and are given in Table 3. The presence of phthalimide end-groups substantially reduced the fluorescence quantum yield of the model compound in comparison to that of AF240 molecule. In the polymers, the collective quenching effects of phthalimide moieties were even more severe, as indicated by more than an order of magnitude reduction in the fluorescence quantum yield in all the polymers. This is most likely due to the restricted mobility of the fluorophore and the quencher as well as their confinement to the same space, increasing the probability of intrachain quenching. It is noteworthy that the intensity reduction was not proportional to the AF240 content. In addition, *o*-benzamide−carboxylic acid moieties in the polymer backbone do not quench fluorescence emission of AF240 fluorophore from the corresponding poly(amic acid) precursors (Figure S-2), confirming the special fluorescence quenching capability of the aromatic imide.[24]

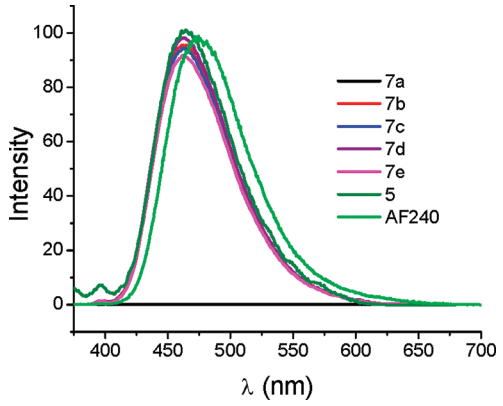

Figure 6. Composite fluorescence spectra of polyimides **7a**−**7e** and the model compound **5** to show their peak positions relative to that of AF240 reference compound. Absorbance at the exciting wavelength of 355 nm was nearly matched at 0.1 for the polymer samples **7a**−**7e**. The data has been normalized for the model compound **5** and AF240 for comparison. Measurements were done in air-saturated toluene.

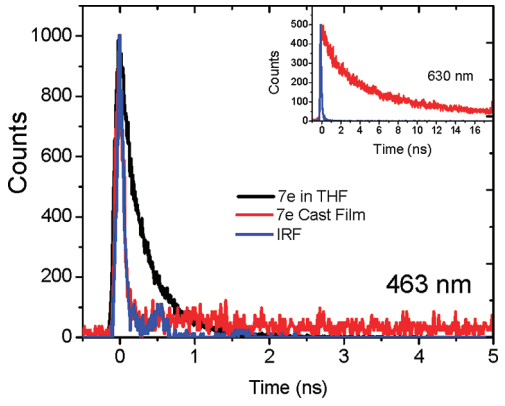

Figure 7. Time-correlated single photon counting data for **7e** in air-saturated THF (black line) and **7e** in a cast film (red line) at 463 nm. Quenching of the emission at 463 nm for the cast film is observed. The inset shows a long-lived emission at 630 nm for the **7e** cast film.

The steady-state emission of the film samples showed a very weak emission (Figure S-3), and the data are cut off due to reabsorption issues of the highly concentrated films. No fluorescence quantum yields of the films were obtained. There is a small amount of emission detected at longer wavelengths around 630 nm that is not seen in the solution data.

Time-correlated single photon counting (TCSPC) measurements were used to determine the singlet excited-state lifetimes of both the solution studies as well as the film samples. Representative data are shown in Figure 7 for polymer **7e** in both THF and as a film, and the lifetimes for all samples are given in Table 3. For the data at the peak maximum of 463 nm, we have observed significant quenching of the singlet excited-state lifetime in the film to within the instrument response function of the TCSPC (~50 ps). The data collected at longer wavelengths (630 nm) for the films shows a long-lived biexponential emission indicating the formation of a new emitting species (Figure 7, inset).

Two-Photon Absorption Cross Sections. The effective (nanosecond) and intrinsic (femtosecond) values of two-photon cross sections ($\sigma^{(2)}$, in the unit of GM = 10^{-50} cm^4 s photon^{-1}) of the CP2-polyimides (**7a**−**7e**) have been determined in THF solutions and film samples, but the model compound (**5**, AF349) determined in THF solution only, by a direct nonlinear transmission (NLT) technique at ~800 nm excitation wavelength. The nonlinear transmission vs input pulse energy plots are shown in Figures S-4 and S-5 of the Supporting Information.

From the results that are summarized in Table 4, we observe that in general both effective and intrinsic $\sigma^{(2)}$ values are directly proportional to the dye content. In other words, an increase in the number density of 2PA chromophoric units does increase the overall 2PA cross section for both effective and intrinsic values. As expected, the effective $\sigma^{(2)}{}_{ns}$ values are more than 2 orders of magnitude larger than the intrinsic $\sigma^{(2)}{}_{fs}$ values because of the contributions from excited-state absorption.[23,40,41,49]

Referring to Table 4, one can see that while $\sigma^{(2)}{}_{fs}$ for the model compound **5** (AF349) is slightly larger than the mean value of AF240s intrinsic cross sections, its effective cross section is only ca. 50% of AF240s value. The latter result could be explained in terms of depleting the excited state population by the phthalimide end-groups (quenching effect) via a nonradiative pathway and, in turn, curtailing the excited-state absorption contributions to the nanosecond 2PA cross section. While both the effective and intrinsic $\sigma^{(2)}$ values of the model compound **5** and the homopolymer **7e** on per repeat unit basis are comparable, the value on per polymer chain basis[42] is much larger for **7e**, with number-averaged (M_n) and weight-averaged (M_w) molecular weights as the lower and upper limits, respectively (see Table S-2).

Phthalimido Effect and Exiplex Formation. When the effective and intrinsic $\sigma^{(2)}$ data obtained for dilute solutions (0.02 M based on FW of each polymer's repeat unit, see Table 1) and those for the cast films are compared in Table 4, it is apparent that whether the test sample is in solution or as a film, there is little or no difference for the data in the femtosecond regime. However, there is consistently a 7- to 9-fold increase in all the film samples in the *nanosecond* results. This is rather surprising when one considers that the extent of ESA contributions to the nanosecond cross section is dependent on the population and lifetime of the excited state. We have initiatially considered the possibility of a nonradiative path involving a photoinduced electron-transfer mechanism, which has been established for phthalimide-based compounds[43] and related polyimides,[44] especially in the presence of photooxidizable molecules such as dimethylaniline.[45] However, such a mechanism would have led to chemical changes and irreversibility such as photoinduced cross-links in polyimides.[44] This apparently did not occur in any of the polymer films **7a**−**7e** as all were still still readily soluble in $CHCl_3$ and THF after 40 min of exposure to UV light (366 nm).

A further probing "fluorophore quencher" experiment was conducted that involved mixing in THF a 1:1 molar mixture of AF240 (light yellow solid) and a faint yellow, nonfluorescent bis(phthalimide) compound (**6**, Scheme 1), *N*,*N*′-{[bis(trifluoromethyl)methylene]di-*p*-phenylene}diphthalimide,[46] prepared from the condensation/imidization reaction of 6FDA and 2 equiv of aniline. The fresh solution was light yellow and highly fluorescent, but after the solvent had been slowly and completely removed in a chemical hood overnight at room temperature, a nonfluorescent solid residue, which had almost identical (orange) color as polymer **7e** film, remained in the vial. Upon adding fresh THF to the resulting solid, a light yellow solution and its "blue-green" fluorescence returned when exposed to a UV lamp (366 nm). This simple experiment suggests that the photoevents involving phthalimide and AF240 are reversible, and the

Table 4. Two-Photon Absorption Properties of Polyimides 7a−7e Measured as Films and THF Solutions at 780 nm (160 fs Pulses) and 800 nm (7 ns Pulses); Experimental Uncertainty Is ±15%[a]

	sample ID						
properties	CP2 (**7a**)	AF349P- 10CP2 (**7b**)	AF349P- 30CP2 (**7c**)	AF349P- 50CP2 (**7d**)	AF349P (**7e**)	AF349[b] (**5**)	AF240 (**2**)
mol % AF240	0	10	30	50	100		
thickness	40 μm	55 μm	65 μm	52 μm	55 μm		
β (cm/GW; fs)	0.0045	0.023	0.042	0.052	0.067		
(cm/GW; ns)	0.6	3.3	6.8	8.8	11		
2PA cross section	solution (0.02 M; THF) data						
$\sigma^{(2)}$ (GM/RU) in fs regime	1.4	7.7	16	23	37	34	17,[c] 45[d]
$\sigma^{(2)}$ (GM/(RU) in ns regime	178	1070	2490	3740	6000	5160	9770
2PA cross section	film data						
σ_2 (GM/RU) in fs regime	0.62	7.7	17.4	27.1	38		
$\sigma^{(2)}$ (GM/(RU) in ns regime	2160	10100	17800	35000	56800		

[a] Abbreviations used in the table: RU = repeat unit; 1 GM (Göppert−Mayer = 1 cm^4 s photon^{-1}). [b] 2PA cross sections are in the unit of GM/molecule. [c] Datum from refs 25 and 35. [d] Datum from ref 49.

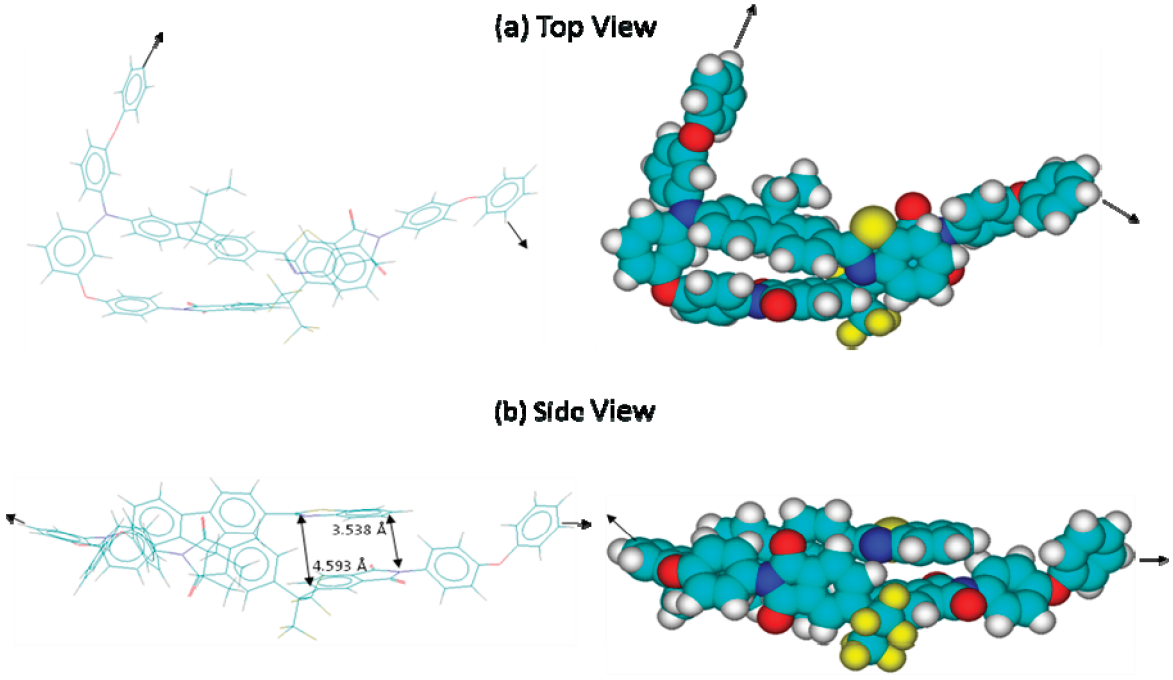

Figure 8. Optimized molecular structure for a repeat unit of polymer **7e** (AF349P) by the MM+ computation method (HyperChem, ver. 7) in stick and space-filled renditions, where the arrows indicate the polymer-chain directions.

orange color of the 1:1 mixture hints that some *intermolecular* structure similar to that of a charge-transfer molecular solid could have formed.

In the solid state, the existence of a phthalimide−AF240 adduct structure, either in interchain or intrachain mode, is possible. Thus, a molecular mechanics (MM) model was utilized to assess these possibilities. Figure 8 depicts a MM-minimized structure that is comprised of a segment containing a repeat unit for **7e**. A striking feature of this structure is the apparent overlapping of the two aromatic heterocycles in an antiparallel fashion (Figure 8a, top view). The mean distance between the phthalimide moiety and the benzobisthiazole end of AF240 structure is ~0.41 nm, which is slightly larger than typical $\pi-\pi$ stacking distance (0.30−0.35 nm), but well below the donor−acceptor distance for through-space energy (FRET range 1−10 nm)[47] processes. Such a close packing arrangement is likely to be driven by the strong interactions between the two planar heterocyles. In addition to dipole−dipole interactions, the fact that (benzo)thiazole is a π-excess system[48] and phthalimide is considered as π-deficient, intermolecular donor−acceptor interactions are probable. Another similarly MM-minimized molecular structure comprised of a copolyimide segment, in which a repeat unit for **7e** (fluorophore) is connected on either end to 3 repeat units and 4 repeat units of CP2-polyimide (**7a,** quencher) seems to confirm the tendency of these two aromatic heterocylces to be close to each other. However, presumably because of the increase in the polymer-chain flexibility provided by the CP2 repeat units, the "interplane" distance becomes larger (mean distance ~0.58 nm), but

Scheme 3. A Proposed Mechanism That Entails (a) Ground-State Structure Resulting from Strong Dipole−Dipole Interaction of Phthalimide and Benzothiazole Moieties, (b) Intramolecular Charge-Transfer Complex Formation, and (c) and Intermolecular but Intrachain Exciplex Formation within the 2PA-Active Fragments in Polyimides 7b−7e[a]

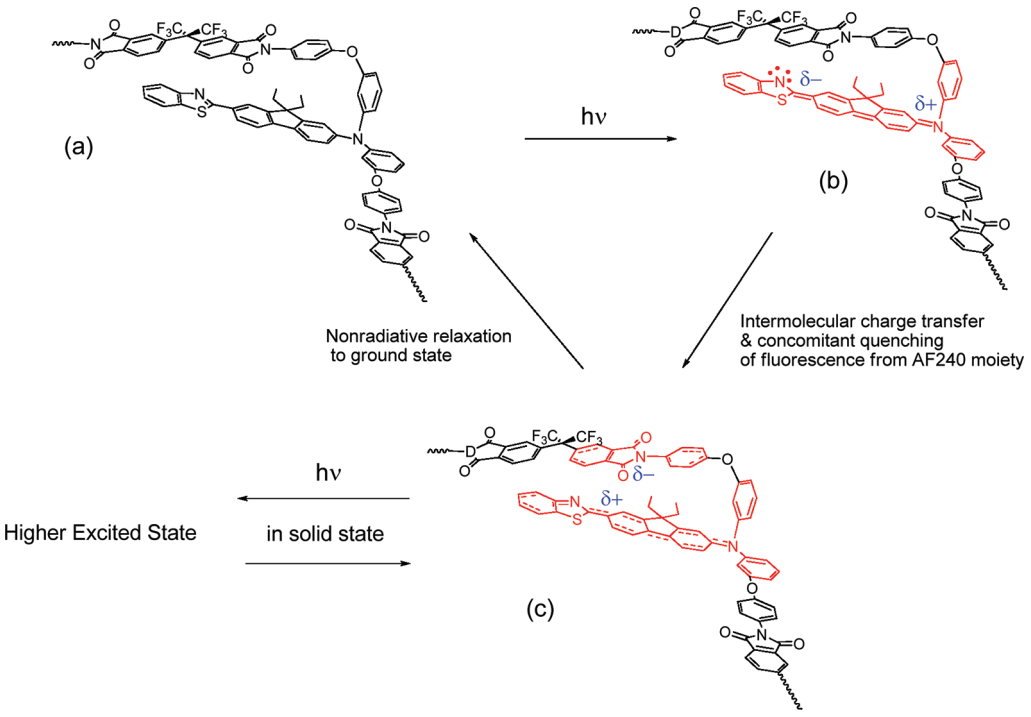

[a] The excited-state structures are shown in red. (Note that the participation of the ether oxygen in the electronic delocalization is unclear, although it is assumed to be marginal because of a meta-substitution pattern.)

still within the range for effective charge or energy transfer (Figure S-6).

On the basis of these results and the fact that the degrees of molecular freedom and mobility are much reduced in polymer films under ambient conditions, we have tentatively concluded that when phthalimide and AF240 moieties are restricted to the molecular confinement defined by the 2PA-active repeat unit of polymers **7b**−**7e**, an *intrachain* supramolecular structure similar to that shown in Figure 8 is preferred. The high solubility of the polyimides **7b**−**7e** also implicates that there are little or no interchain interactions (physical cross-linking via interchain charge-tranfer complexation) present. Thus, it follows that this confined supramolecular arrangement may account for the substantially larger enhancement in the *nanosecond* two-photon response in the **7b**−**7e** polymer films than the corresponding dilute solutions.

Thus, we propose a working mechanism as shown in Scheme 3 to visualize the photophysical events likely to occur in these polymer films. Briefly, structure (a) represents the ground-state molecular arrangement of the 2PA-active repeat unit. The formation of structure (a) is driven by only strong dipole−dipole interactions, not charge-transfer-type interaction, which is ruled out by the lack of absorption evidence (i.e., some indication of a red-shifted charge transfer band). Upon excitation under either one- or two-photon conditions, an intramolecular charge transfer within the AF-240 moiety instantaneously occurs. The benzothiazole-end is now more electron-rich, and with the electron-deficient phthalimide (most likely still in ground state) moiety nearby, they form an exciplex that quenches the fluorescence emission of the excited AF240 moiety. This exciplex has a lifetime (∼10 ns; Table 3) on the same order as the nanosecond laser pulses (∼8 ns). Consequently, it could absorb additional photons, resulting in an enhancement of the effective 2PA cross section. However, in solution the lifetime (∼0.4 ns) of this exciplex is much shorter than the laser pulse duration, and hence, no enhancement was observed. The existence of the exciplex appears to be supported by the appearance of a new, but weak, fluorescence band peaked at ∼629−632 nm for all polymer films **7b**−**7e**, which was absent in CP2−polyimide (**7a**) film (Figure S-3). This band is red-shifted by ∼166−176 nm from the fluorescence band (463 nm) observed for all the polymer solution samples (see Table 3).

■ CONCLUSIONS

Based on the notion that a two-photon active, *amorphous* polymer is a viable approach to increasing the chromophore number density and, in turn, the overall 2PA response, a series of organo-soluble 6FDA-based polyimides possessing composition-variable, 2PA sensitivity upon excitation at NIR wavelength of ∼800 nm have been synthesized. Our results indicate that the covalently bound phthalimide functionality can drastically quench the fluorescence emission from the AF240 segments of these polymers as well as the model compound (AF349) in solution and film samples. Fluorescence quenching does not diminish their two-photon sensitivities on both nanosecond and femtosecond time scales in solution. On the contrary, in the solid state, the supramolecular interactions of the phthalimide and the AF240 moieties in the polymer chain have actually resulted in up to nearly an order of magnitude increase in *nanosecond* 2PA response. Since this enhancement occurs only on the nanosecond

time scale and excited-state absorption contributes to the effective 2PA cross-section measured, based on the evidence presented in this work, we propose that a new excited species (an intrachain exciplex) with a lifetime on the order of 10 ns is responsible. Further work to define the scope and extent of solid-state nanosecond enhancement in this polyimide and related polymer systems is currently underway.

■ ASSOCIATED CONTENT

Supporting Information. (i) Table S-1: density values and corresponding 2PA dye concentrations for polyimide films; (ii) Table S-2: two-photon absorption cross-section values (GM) of polyimides **7a**−**7e**, model compound (AF349), and AF240, measured at 780 nm (160 fs pulses) and 800 nm (7 ns pulses) separately in THF (0.02 M; 1 cm cuvette); experimental uncertainty is ±15%; (iii) Figure S-1: plot of log(MW) vs log(η) for the series of copolymers; (iv) Figure S-2: 90/10 copolymer in amic acid precursor and imide (**7b**) forms in $CDCl_3$, digital photo (left) taken without exposure to a hand-held TLC UV-lamp (254 nm; under room conditions) and (right) upon the exposure to same UV-light source; (v) Figure S-3: emission spectra of polymer films **7a**−**7e** that were excited at 400 nm using a front-face geometry to eliminate any inner filter effects that may be caused by high absorbance at the exciting wavelength, data are extremely noisy but show a new emission in the 600 nm region; (vi) Figure S-4: nonlinear transmission of polymers **7a**−**7e** and model compound (**5**; AF349) measured in THF solutions and in fs regime; (vii) Figure S-5: nonlinear transmission of polymer **7a**−**7e** and model compound (**5**; AF349) measured in THF solutions and in ns-regime; (viii) Figure S-6: MM-minimized molecular structure to represent a segment for polymers **7b**−**7c** that is made up a repeat unit of AF-349P (polymer **7e**) connected to 3 repeat units of CP2 (polymer **7a**) on one side and 4 repeat units of CP2 on the other side; (ix) proton and C-13 NMR spectra with tentative assignments for the compounds related to this work. This material is available free of charge via the Internet at http://pubs.acs.org.

■ AUTHOR INFORMATION

Corresponding Author

*E-mail: loon-seng.tan@wpafb.af.mil; Ph 937-255-9153.

■ ACKNOWLEDGMENT

We thank Marlene Houtz (University of Dayton Research Institute) for TGA and DSC data. Funding support was provided by Materials & Manufacturing Directorate & Office of Scientific Research (AFOSR), Air Force Research Laboratory.

■ REFERENCES

(1) Göppert-Mayer, M. *Ann. Phys. (Leipzig)* **1931**, *9*, 273–294.
(2) Kaiser, W.; Garret, C. G. B. *Phys. Rev. Lett.* **1961**, *7*, 229–231.
(3) (a) Reinhardt, B. A. *Trends Polym. Sci. (Cambridge, U. K.)* **1996**, *4*, 287–289. (b) *Trends Polym. Sci. (Cambridge, U. K.)* **1993**, *1*, 4–9. (c) Reinhardt, B. A.; Unroe, M. R.; Evers, R. C.; Zhao, M.; Samoc, M.; Prasad, P. N.; Sinsky, M. *Chem. Mater.* **1991**, *3*, 864–71. (d) Zhao, M.; Samoc, M.; Prasad, P. N.; Reinhardt, B. A.; Unroe, Marilyn, R.; Prazak, M.; Evers, R. C.; Kane, J. J.; Jariwala, C.; Sinsky, M. *Chem. Mater.* **1990**, *2*, 670–8. (e) Zhao, M.; Cui, Y.; Samoc, M.; Prasad, P. N.; Unroe, M. R.; Reinhardt, B. A. *J. Chem. Phys.* **1991**, *95*, 3991–4001. (f) Said, A. A.; Wamsley, C.; Hagan, D. J.; Van Stryland, E. W.; Reinhardt, B. A.; Roderer, P.; Dillard, A. G. *Chem. Phys. Lett.* **1994**, *228*, 646–650.
(4) Kano, H.; Kawata, S. *Opt. Lett.* **1996**, *21*, 1848–1850.
(5) (a) Jung, J.-M.; Yoo, H.-W.; Stellacci, F.; Jung, H.-T. *Adv. Mater.* **2010**, *22*, 2542–2546. (b) Mendonca, C. R.; Kandyla, M.; Shih, T.; Aroca, R. F.; Constantino, C. J. L.; Mazur, E. *Appl. Phys. A: Mater. Sci. Process* **2009**, *96*, 369–372. (c) Cohanoschi, I.; Yao, S.; Belfield, K. D.; Hernandez, F. E. *J. Appl. Phys.* **2007**, *101*, 086112/1–086112/3. (d) He, R.-Y.; Su, Y.-D.; Cho, K.-C.; Lin, C.-Y.; Chang, N.-S.; Chang, C.-H.; Chen, S.-J. *Opt. Express* **2009**, *17*, 5987–5997. (e) Gryczynski, I.; Malicka, J.; Lakowicz, J. R.; Goldys, E. M.; Calander, N.; Gryczynski, Z. *Thin Solid Films* **2005**, *491*, 173–176. (f) Cohanoschi, I.; Hernandez, F. E. *J. Phys. Chem. B* **2005**, *109*, 14506–14512. (g) Wenseleers, W.; Stellacci, F.; Meyer-Friedrichsen, T.; Mangel, T.; Bauer, C. A.; Pond, S. J. K.; Marder, S. R.; Perry, J. W. *J. Phys. Chem. B* **2002**, *106*, 6853–6863. (h) Campbell, B.; Lei, J.; Kiaei, D.; Sustarsic, D.; El Shami, S. *Clin. Chem.* **2004**, *50*, 1942–1943.
(6) (a) Strehmel, B.; Strehmel, V. *Adv. Photochem.* **2007**, *29*, 111–354. (b) He, G. S.; Tan, L.-S.; Zheng, Q.; Prasad, P. N. *Chem. Rev.* **2008**, *108*, 1245–1330. (c) Terenziani, F.; Katan, C.; Badaeva, E.; Tretiak, S.; Blanchard-Desce, M. *Adv. Mater.* **2008**, *20*, 4641–4678. (d) Rumi, M.; Barlow, S.; Wang, J.; Perry, J. W.; Marder, S. R. *Adv. Polym. Sci.* **2008**, *213*, 1–95. (e) Belfield, K. D.; Yao, S.; Bondar, M. V. *Adv. Polym. Sci.* **2008**, *213*, 97–156. (f) Pawlicki, M.; Collins, H. A.; Denning, R. G.; Anderson, H. L. *Angew. Chem., Int. Ed.* **2009**, *48*, 3244–3266. (g) Kim, H. M.; Cho, B. R. *Chem. Commun.* **2009**, 153–164. (h) Aratani, N.; Kim, D.; Osuka, A. *Chem.—Asian J.* **2009**, *4*, 1172–1182. (h) Iyoda, M. *Pure Appl. Chem.* **2010**, *82*, 831–841.
(7) (a) Lee, K.-S.; Kim, R. H.; Yang, D.-Y.; Park, S. H. *Prog. Polym. Sci.* **2008**, *33*, 631–681. (b) Sun, H.-B.; Kawata, S. *Adv. Polym. Sci.* **2004**, *170*, 169–273. (c) Kawata, S.; Sun, H.-B. *Appl. Surf. Sci.* **2003**, *208*−*209*, 153–158. (d) Jhaveri, S. J.; McMullen, J. D.; Sijbesma, R.; Tan, L.-S.; Zipfel, W.; Ober, C. K. *Chem. Mater.* **2009**, *21*, 2003–2006.
(8) Ford, P. C. *Acc. Chem. Res.* **2008**, *41*, 190–200.
(9) Two-photon absorbing dendrimers: (a) Wan, Y.; Yan, L.; Zhao, Z.; Ma, X.; Guo, Q.; Jia, M.; Lu, P.; Ramos-Ortiz, G.; Maldonado, J. L.; Rodriguez, M.; Xia, A. *J. Phys. Chem. B* **2010**, *114*, 11737–11745. (b) Xu, B.; Fang, H.-H.; Chen, F.-P.; Lu, H.-G.; He, J.-T.; Li, Y.-W.; Chen, Q.-D.; Sun, H.-B.; Tian, W.-J. *New J. Chem.* **2009**, *33*, 2457–2464. (c) Mongin, O.; Krishna, T. R.; Werts, M. H. V.; Caminade, A.-M.; Majoral, J.-P.; Blanchard-Desce, M. *Chem. Commun.* **2006**, 915–917. (d) Drobizhev, M.; Karotki, A.; Dzenis, Y.; Rebane, A.; Suo, Z.; Spangler, C. W. *J. Phys. Chem. B* **2003**, *107*, 7540–7543.
(10) Two-photon absorbing hyperbranched polymers: (a) Zou, L.; Liu, Y.; Ma, N.; Macoas, E.; Martinho, J. M. G.; Pettersson, M.; Chen, X.; Qin, J. *Phys. Chem. Chem. Phys.* **2011**, *13*, 8838–8846. (b) Jiang, Y.-H.; Wang, Y.-C.; Yang, J.-B.; Hua, J.-L.; Wang, B.; Qian, S.-Q.; Tian, H. *J. Polym. Sci., Part A: Polym. Chem.* **2011**, *49*, 1830–1839. (c) Jiang, Y.; Wang, Y.; Hua, J.; Qu, S.; Qian, S.; Tian, H. *J. Polym. Sci., Part A: Polym. Chem.* **2009**, *47*, 4400–4408. (d) Qin, A.; Lam, J. W. Y.; Dong, H.; Lu, W.; Jim, C. K. W.; Dong, Y.; Haeussler, M.; Sung, H. H. Y.; Williams, I. D.; Wong, G. K. L.; Tang, B. Z. *Macromolecules* **2007**, *40*, 4879–4886. (e) Li, C.; Liu, C.; Li, Q.; Gong, Q. *Chem. Phys. Lett.* **2004**, *400*, 569–572. (f) Hua, J. L.; Li, B.; Meng, F. S.; Ding, F.; Qian, S. X.; Tian, H. *Polymer* **2004**, *45*, 7143–7149.
(11) (a) Belfield, K. D.; Reinhardt, B. A.; Brott, L. L.; Clarson, S. J.; Najjar, O.; Pius, S. M.; Van Stryland, E. W.; Negres, R. *Polym. Prepr.* **1999**, *40* (1), 127–128. (b) Wang, D.; Zhou, G. Y.; Ren, Y.; Yu, X. Q.; Cheng, X. F.; Yang, S. J.; Xu, X. G.; Shao, Z. S.; Jiang, M. H. *Solid State Commun.* **2002**, *121*, 339–344. (c) Chung, S.-J.; Maciel, G. S.; Pudavar, H. E.; Lin, T.-C.; He, G. S.; Swiatkiewicz, J.; Prasad, P. N.; Lee, D. W.; Jin, J.-I. *J. Phys. Chem. A* **2002**, *106*, 7512–7520. (d) Oztemiz, S.; Jobanputra, M. C.; Clarson, S. J. *Polym. Prepr.* **2003**, *44* (1), 1165–1166. (e) Belfield, K. D.; Morales, A. R.; Hales, J. M.; Hagan, D. J.; Van Stryland, E. W.; Chapela, V. M.; Percino, J. *Chem. Mater.* **2004**, *16*, 2267–2273. (f) Belfield, K. D.; Yao, S.; Morales, A. R.; Hales, J. M.; Hagan, D. J.; Van Stryland, E. W.; Chapela, V. M.; Percino, J. *Polym. Adv. Technol.* **2005**, *16*, 150–155. (g) Qin, A.; Jim, C. K. W.; Lu, W.; Lam, J. W. Y.;

Haeussler, M.; Dong, Y.; Sung, H. H. Y.; Williams, I. D.; Wong, G. K. L.; Tang, B. Z. *Macromolecules* **2007**, *40*, 2308–2317. (h) Huang, F.; Tian, Y.; Chen, C.-Y.; Cheng, Y.-J.; Young, A. C.; Jen, A. K.-Y. *J. Phys. Chem. C* **2007**, *111*, 10673–10681. (i) *eXPRESS Polym. Lett.* **2007**, *1*, 482–487. (j) Manoj, N.; Muhammad, H.; Xu, Q.; Valiyaveettil, S. *Macromolecules* **2008**, *41*, 8473–8482. (k) Zhang, H.; Guo, E.; Zhang, X.; Yang, W. *J. Polym. Sci., A Polym. Chem.* **2010**, *48*, 463–470. (l) Hegde, P. K.; Adhikari, A. V.; Manjunatha, M. G.; Sandeep, C. S. S.; Philip, R. *J. Appl. Polym. Sci.* **2010**, *117*, 2641–2650. (m) Huang, X.; Shi, Q.; Chen, W.-Q.; Zhu, C.; Zhou, W.; Zhao, Z.; Duan, X.-M.; Zhan, X. *Macromolecules* **2010**, *43*, 9620–9626. (n) Wang, H.; Li, Z.; Shao, P.; Qin, J.; Huang, Z.-L. *J. Phys. Chem. B* **2010**, *114*, 22–27. (o) Goudreault, T.; He, Z.; Guo, Y.; Ho, C.-L.; Zhan, H.; Wang, Q.; Ho, K. Y.-F.; Wong, K.-L.; Fortin, D.; Yao, B.; Xie, Z.; Wang, L.; Kwok, W.-M.; Harvey, P. D.; Wong, W.-Y. *Macromolecules* **2010**, *43*, 7936–7949. (p) Jiang, Y.-H.; Wang, Y.-C.; Yang, J.-B.; Hua, J.-L.; Wang, B.; Qian, S.-Q.; Tian, H. *J. Polym. Sci., Part A: Polym. Chem.* **2011**, *49*, 1830–1839.

(12) Hergenrother, P. M. *High Perform. Polym.* **2003**, *15*, 3–45.

(13) Sroog, C. E. *Prog. Polym. Sci.* **1991**, *16*, 561–694.

(14) (a) de Abajo, J.; de la Campa, J. G.; Lozano, A. E.; Espeso, J.; Garcia, C. *Macromol. Symp.* **2003**, *199*, 293–305. (b) Al-Masri, M.; Fritsch, D.; Kricheldorf, H. R. *Macromolecules* **2000**, *33*, 7127–7135. (c) Fang, J.; Kita, H.; Okamoto, K.-i. *Macromolecules* **2000**, *33*, 4639–4646.

(15) Fukukawa, K.-i.; Ueda, M. *J. Photopolym. Sci.* **2009**, *22*, 761–771.

(16) Wong, C. P. *Polymers for Electronic & Photonic Applications*; Academic Press: London, 1993.

(17) (a) Kim, T.-D.; Lee, K.-S.; Lee, G. U.; Kim, O.-K. *Polymer* **2000**, *41*, 5237–5245. (b) Liu, Y.-G.; Sui, Y.; Yin, J.; Gao, J.; Zhu, Z.-K.; Huang, D.-Y.; Wang, Z.-G. *J. Appl. Polym. Sci.* **2000**, *76*, 290–295. (c) Lu, J.; Yin, J. *J. Polym. Sci., Part A: Polym. Chem.* **2003**, *41*, 303–312. (d) Park, S. K.; Do, J. Y.; Ju, J. J.; Park, S.; Kim, M.; Lee, M.-H. *React. Funct. Polym.* **2006**, *66*, 974–983. (e) Qiu, F.; Da, Z.; Yang, D.; Cao, G.; Li, P. *Dyes Pigm.* **2008**, *77*, 564–569.

(18) (a) Jen, A. K. Y.; Liu, Y.; Zheng, L.; Liu, S.; Drost, K. J.; Zhang, Y.; Dalton, L. R. *Adv. Mater.* **1999**, *11*, 452–455. (b) Chen, T.-A.; Jen, A. K. Y.; Cai, Y. *Macromolecules* **1996**, *29*, 535–539. (c) Chen, T.-A.; Jen, A. K. Y.; Cai, Y. *J. Am. Chem. Soc.* **1995**, *117* (27), 7295–7296.

(19) (a) Sekkat, Z.; Wood, J.; Knoll, W.; Volksen, W.; Miller, R. D.; Knoesen, A. *J. Opt. Soc. Am. B* **1997**, *14*, 829–833. (b) Chen, J. P.; Lagugne-Labarthet, F.; Natansohn, A.; Rochon, P. *Macromolecules* **1999**, *32*, 8572–8579. (c) Si, J.; Mitsuyu, T.; Ye, P.; Li, Zh.; Shen, Y.; Hirao, K. *Opt. Commun.* **1998**, *147*, 313–316. (d) Meng, X.; Natansohn, A.; Rochon, P. *Polymer* **1997**, *38*, 2677–2682. (e) Sava, I.; Resmerita, A.-M.; Lisa, G.; Damian, V.; Hurduc, N. *Polymer* **2008**, *49*, 1475–1482.

(20) Schab-Balcerzak, E.; Siwy, M.; Kawalec, M.; Sobolewska, A.; Chamera, A.; Miniewicz, A. *J. Phys. Chem A* **2009**, *113*, 8765–8780.

(21) Two-photon properties were reported only recently for certain mixed aliphatic−aromatic poly(ester-imides). See: Siwy, M.; Jarzabek, B.; Switkowski, K.; Pura, B.; Schab-Balcerzak, E. *Polym. J.* **2008**, *40*, 813–824.

(22) Ehrlich, J. E.; Wu, X.-L.; Lee, I.-Y. S.; Hu, Z.-Y.; Rockel, H.; Marder, S. R.; Beljonne, D.; Bredas, J.-L. *Opt. Lett.* **1997**, *22*, 1843–1845.

(23) (a) Sutherland, R. L.; Brant, M. C.; Heinrichs, J.; Rogers, J. E.; Slagle, J. E.; McLean, D. G.; Fleitz, P. A. *J. Opt. Soc. Am. B* **2005**, *22*, 1939–1948.(b) Sutherland, R. L.; McLean, D. G.; Brant, M. C.; Rogers, J. E.; Fleitz, P. A.; Urbas, A. M., *Proc. SPIE—Int. Soc. Opt. Eng.* **2006**, *6330* (Nonlinear Optical Transmission and Multiphoton Processes in Organics IV), 633006/1−633006/15

(24) (a) Hasegawa, M.; Horie, K. *Prog. Polym. Sci.* **2001**, *26*, 259. (b) Hrdlovič, P. *Polym. News* **2004**, *29*, 50–60.

(25) Kannan, R.; He, G. S.; Yuan, L.; Xu, F.; Prasad, P. N.; Dombroskie, A. G.; Reinhardt, B. A.; Baur, J. W.; Vaia, R. A.; Tan, L.-S. *Chem. Mater.* **2001**, *13*, 1896–1904.

(26) CP2 is shortened from the original acronym, LaRC-CP2, which originated from a NASA research program on colorless polyimides (CP) for coating applications, where optical transparency was critical: (a) St. Clair, A. K.; St. Clair, T. L.; Shevket, K. I. *Polym. Mater. Sci. Eng.* **1984**, *51*, 62–66. (b) Miner, G. A.; Stoakley, D. M.; St. Clair, A. K.; Gierow, P. A.; Bates, K. *Polym. Mater. Sci. Eng.* **1997**, *76*, 381–382.

(27) ManTech SRS Technologies. Technical bulletin, "LaRC-CP1 and LaRC-CP2 polyimide film properties", 2004; http://www.mantechmaterials.com.

(28) Gosh, M. K., Mittal, K. L. *Polyimides: Fundamentals and Applications*; Marcel Dekker: New York, 1996.

(29) Rogers, J. E.; Cooper, T. M.; Fleitz, P. A.; Glass, D. J.; McLean, D. G. *J. Phys. Chem. A* **2002**, *106*, 10108–10115.

(30) Demas, J. N.; Crosby, G. A. *J. Phys. Chem.* **1971**, *75*, 991–1024.

(31) For a similar femtosecond 2PA cross-section measurement setup, see: He, G. S.; Swiatkiewicz, J.; Jiang, Y.; Prasad, P. N.; Reinhardt, B. A.; Tan, L.-S.; Kannan, R. *J. Phys. Chem. A* **2000**, *104*, 4805–4810.

(32) He, G. S.; Yuan, L.; Cheng, N.; Bhawalkar, J. D.; Prasad, P. N.; Brott, L. L.; Clarson, S. J.; Reinhardt, B. A. *J. Opt. Soc. Am. B* **1997**, *14*, 1079–1087.

(33) He, G. S.; Lin, T.-C.; Dai, J.; Prasad, P. N.; Kannan, R.; Dombroskie, A, G.; Vaia, R. A.; Tan, L.-S. *J. Chem. Phys.* **2004**, *120*, 5275–5284.

(34) Baev, A.; Salek, P.; Gel'mukhanov, F.; Aagren, H. *J. Phys. Chem. B* **2006**, *110*, 5379–5385.

(35) Das, G. P.; Yeates, A. T.; Dudis, D. S. *Int. J. Quantum Chem.* **2000**, *80*, 1039–1042.

(36) For the homopolyimide (parent) containing AF240 moiety in every repeat unit, it is designated as AF349P. For the designation of the copolyimides, the central 2-digit number refers to the mol % of AF240 component in the copolymer; e.g., in AF349P-10CP2, 10 mol% of dye is formally present in the polymer chain.

(37) The film density of CP2 is reported to be 1.43 g/cm^3. See: Espuche, E.; David, L.; Afeld, J. L.; Compton, J. M.; Kranbuehl, D. E. *Macromol. Symp.* **2005**, *228*, 155–165.

(38) March, J. *Advanced Organic Chemistry: Reactions, Mechanisms & Structures*, 4th ed.; Wiley: New York, 1992; p 280.

(39) (a) Nguyen, K. A.; Rogers, J. E.; Slagle, J. E.; Day, P. N.; Kannan, R.; Tan, L.-S.; Fleitz, P. A.; Pachter, R. *J. Phys. Chem. A* **2006**, *110*, 13172–13182. (b) Nguyen, K. A.; Day, P. N.; Pachter, R. *Theor. Chem. Acc.* **2008**, *120*, 167–175.

(40) Li, C.; Yang, K.; Feng, Y.; Su, X.; Yang, J.; Jin, X.; Shui, M.; Wang, Y.; Zhang, X.; Song, Y.; Xu, H. *J. Phys. Chem. B* **2009**, *113*, 15730–15733.

(41) Swiatkiewicz, J.; Prasad, P. N.; Reinhardt, B. A. *Opt. Commun.* **1998**, *157*, 135–138.

(42) For multiphoton applications such as multiphoton fluorescence quenching for chemical sensing, which requires conjugated polymer to be sufficiently high molecular weight, the two-photon cross-sections are reported on the per entire-chain basis. See for example: Narayanan, A.; Varnavski, O. P.; Swager, T. M.; Goodson, T., III *J. Phys. Chem. C* **2008**, *112*, 881–884.

(43) (a) Oelgemoller, M.; Griesbeck, A. G. *J. Photochem. Photobiol., C* **2002**, *3*, 109–127. (b) Griesbeck, A. G.; Schieffer, S. *Photochem. Photobiol. Sci.* **2003**, *2*, 113–117. (c) Griesbeck, A. G.; Gorner, H. *J. Photochem. Photobiol., A* **1999**, *129*, 111–119.

(44) Li, W.; Fox, M. A. *J. Phys. Chem. B* **1997**, *101*, 11068–11076.

(45) Freilich, S. C. *Macromolecules* **1987**, *20*, 973–978.

(46) (a) Li, Y.; Wang, Z. *Acta Crystallogr., Sect. E: Struct. Rep. Online* **2008**, *E64* (2), o388/1–o388/8. (b) Naitoh, K.; Ishii, K.; Yamaoka, T.; Omote, T. *Polym. Adv. Technol.* **1993**, *4*, 294–301.

(47) Hillisch, A.; Lorenz, M.; Diekmann, S. *Curr. Opin. Struct. Biol.* **2001**, *11*, 201–207.

(48) Newkome, G. R.; Paudler, W. W. *Contemporary Heterocyclic Chemistry*; Wiley-Interscience: New York, 1982; Chapter 4.

(49) Rogers, J. E.; Slagle, J. E.; McLean, D. G.; Sutherland, R. L.; Brant, M. C.; Heinrichs, J.; Jakubiak, R.; Kannan, R.; Tan, L.-S.; Fleitz, P. A. *J. Phys. Chem. A* **2007**, *111*, 1899–1906.